

01-201

# Environment Canada

## Water Science and Technology Directorate

---

Direction générale des sciences  
et de la technologie, eau

# Environnement Canada

TD  
226  
N87  
no.  
01-201

Acid Neutralization Mechanisms and Metal Release  
in Mine Tailings

By

J. Jurjovec, C. Ptacek, D. Blowes

NWRI Contribution # 01-201

01-201

## **Acid Neutralization Mechanisms and Metal Release in Mine Tailings**

Jurjovec, J., Ptacek, C.J. and Blowes, D.W.

### **MANAGEMENT PERSPECTIVE**

This work supports the ESD Issue Conserving Canada's Ecosystems and the Business Plan Deliverable Nature.

Migration of acid and metals from mine tailings is a severe problem in Canada and the world. Mine tailings are the finely ground sulfides and gangue minerals that are of insufficient value for further processing. Tailings are typically stored in piles or impoundments at mine sites where they are allowed to come in contact with atmospheric oxygen. As a result, sulfide minerals in the tailings oxidize, releasing acid and metals to the environment. Some of the acid is neutralized by gangue minerals (carbonates, aluminosilicates) contained in the tailings. Eventually the neutralization capacity can be consumed (years to decades), allowing the acid to migrate from the site. Under low pH conditions, many metals are mobilized resulting in large loadings of metals to groundwaters and surface waters. At many sites in Canada, the acid fronts will first reach the water table and will discharge to surface water bodies over the next several decades or longer. This paper describes a method developed to accurately quantify acid neutralization reactions under flow conditions representative of those occurring in the field. The results will assist in predicting the arrival time of acidic fronts in mine wastes in general. This information will assist in planning for the extremely large acid and metal loadings expected to occur over the next several decades or longer.

This paper represents part I of a three-part series on this topic. The next steps will be directed at developing an accurate model which incorporates dissolution kinetics for a range of minerals contributing to the acid neutralization reactions in tailings.

## **Mécanismes de neutralisation des acides et dégagement de métaux dans les résidus miniers**

Par

Jurjovec, J., Ptacek, C.J. et Blowes, D.W.

### **RÉSUMÉ À L'INTENTION DE LA DIRECTION**

Ce travail contribue à l'activité de la DGSE Conservation des écosystèmes au Canada, et contribue au secteur d'activités de la nature.

La migration des acides et des métaux hors des résidus miniers est un grave problème au Canada et ailleurs dans le monde. Les résidus miniers sont constitués des sulfures finement broyés et des minéraux formant la gangue et n'ayant pas assez de valeur pour justifier leur traitement. Ordinairement, les résidus sont empilés ou déposés dans des bassins d'accumulation sur le terrain des mines, où ils sont exposés à l'oxygène atmosphérique. Il s'ensuit que les minéraux sulfurés s'oxydent et libèrent des acides et des métaux dans le milieu. Ces acides sont en partie neutralisés par les minéraux de la gangue (carbonates, aluminosilicates) contenue dans les résidus. Éventuellement, le pouvoir de neutralisation s'épuise (c'est une question d'années ou de décennies) et les acides migrent hors du site. À bas pH, de nombreux métaux sont libérés et sont à l'origine d'une forte charge dans les eaux souterraines ou de surface. À de nombreux sites canadiens, le front acide atteindra la nappe d'eau avant de passer dans des masses d'eau de surface au cours des quelques décennies suivantes ou plus. Ce rapport fait état d'une méthode mise au point pour quantifier avec exactitude les réactions de neutralisation des acides dans des conditions d'écoulement de l'eau représentatives de celles observées sur le terrain. Cela nous aidera à prévoir l'arrivée des fronts acides des résidus miniers en général. Les renseignements obtenus contribueront à la planification nécessaire pour contrer les charges très élevées d'acides et de métaux qu'on devrait observer au cours des quelques décennies à venir ou plus.

Cet article est le premier de trois articles traitant de ce sujet. Les travaux subséquents porteront sur l'élaboration d'un modèle exact qui incorporera des équations de cinétique de la dissolution en fonction de différents minéraux contribuant aux réactions de neutralisation des acides dans les résidus.

## RÉSUMÉ

L'exploitation des gisements de métaux communs et les opération de concentration peuvent donner lieu au dégagement de métaux dans le milieu. Lorsqu'ils sont exposés à l'oxygène et à l'eau, les minéraux sulfurés qui sont contenus dans les résidus sont oxydés et se dissolvent. Deux principaux processus géochimiques antagonistes agissent sur la migration des métaux dissous dans les bassins d'accumulation des résidus miniers, soit l'oxydation des sulfures et la neutralisation des acides. L'étude porte spécialement sur les réactions de neutralisation des acides qui se produisent dans la zone saturée des bassins d'accumulation des résidus miniers. De manière à simuler les conditions prédominant dans de nombreux bassins d'accumulation des résidus miniers, nous avons fait circuler continuellement de l'acide sulfurique à 0,1 M dans des colonnes contenant des résidus frais et non oxydés. Cette expérience nous fournit des séries temporelles d'observations détaillées du pH, de l'Eh et des concentrations de métaux. Les résultats obtenus sont conformes à des observations antérieures sur le terrain suggérant qu'une série de réactions de dissolution et de précipitation minérales déterminent le pH et le degré de mobilité des métaux. Ordinairement, cette série consiste en des minéraux carbonatés, des hydroxydes d'Al et de Fe(III) et des aluminosilicates. Dans le cas des résidus miniers de Kidd Creek, la série de dissolution est constituée d'ankérite-dolomite, de sidérite, de gibbsite et d'aluminosilicates. Dans l'expérience sur colonne, trois plateaux distincts de pH ont été observés : 5,7, 4,0 et 1,3. Nous avons observé un lien entre le dégagement d'éléments à l'état de traces, comme le Cd, le Co, le Cr, le Cu, le Li, le Ni, le Pb le V et le Zn, et les zones tampons de pH. La concentration du Zn, du Ni et du Co est élevée au premier plateau (pH de 7,5) tandis que le Cd, le Cr, le Pb, l'As, le V et l'Al sont libérés lorsque le pH de l'eau de porosité passe à 4,0 ou moins.



## Acid neutralization mechanisms and metal release in mine tailings: A laboratory column experiment

JASNA JURIOVEC,<sup>1,\*</sup> CAROL J. PEACEK,<sup>1,2</sup> and DAVID W. BLOWES<sup>1</sup>

<sup>1</sup>Department of Earth Sciences, University of Waterloo, Waterloo, ON N2L 3G1, Canada

<sup>2</sup>National Water Research Institute, Burlington, ON L7R 4A6, Canada

(Received July 13, 2001; accepted in revised form November 26, 2001)

**Abstract**—Mining and milling of base metal ore deposits can result in the release of metals to the environment. When sulfide minerals contained in mine tailings are exposed to oxygen and water, they oxidize and dissolve. Two principal antagonistic geochemical processes affect the migration of dissolved metals in tailings impoundments: sulfide oxidation and acid neutralization. This study focuses on acid neutralization reactions occurring in the saturated zone of tailings impoundments. To simulate conditions prevailing in many tailings impoundments, 0.1 mol/L sulfuric acid was passed continuously through columns containing fresh, unoxidized tailings, collected at Kidd Creek metallurgical site. The results of this column experiment represent a detailed temporal observation of pH, Eh, and metal concentrations. The results are consistent with previous field observations, which suggest that a series of mineral dissolution-precipitation reactions control pH and metal mobility. Typically, the series consists of carbonate minerals, Al and Fe(III) hydroxides, and aluminosilicates. In the case of Kidd Creek tailings, the dissolution series consists of ankerite-dolomite, siderite, gibbsite, and aluminosilicates. In the column experiment, three distinct pH plateaus were observed: 5.7, 4.0, and 1.3. The releases of trace elements such as Cd, Co, Cr, Cu, Li, Ni, Pb, V, and Zn were observed to be related to the pH buffering zones. High concentrations of Zn, Ni, and Co were observed at the first pH plateau (pH 5.7), whereas Cd, Cr, Pb, As, V, and Al were released as the pH of the pore water decreased to 4.0 or less. Copyright © 2002 Elsevier Science Ltd

### 1. INTRODUCTION

Mining and milling of sulfide ore generates large quantities of waste rock and finely crushed mill tailings, which generate acidic effluents due to weathering under atmospheric conditions. Acidic waters generated in the unsaturated zone of tailings impoundments contain elevated concentrations of Fe, SO<sub>4</sub>, and potentially toxic metals. According to U.S. Environmental Protection Agency (1994) reports, metal loadings from mine wastes cause environmental damage that is far greater than the effect of the pH of the water released from mine wastes. Therefore, understanding the mechanisms controlling the mobility of metals in the pore water of mill tailings is crucial in the prediction, remediation, and prevention of these problems.

Field observations suggest that metal mobility depends on pH of the tailings pore water (Dubrovsky et al., 1985; Morin et al., 1988; Blowes, 1990). The chief cause of acidic waters, the abiotic and biotic oxidation of pyrite and ferrous iron, has been studied extensively for more than 30 yr, including the conditions and parameters that promote the oxidation reaction (Singer and Stumm, 1970; Nicholson et al., 1988; Moses and Herman, 1991). Much less has been written about acid neutralization, a beneficial process occurring in mill tailings.

Studies of uranium tailings at the abandoned Nordic Main impoundment near Elliot Lake, Ontario, indicate that the mobility of most of solutes in the tailings (Dubrovsky et al., 1985) and in the underlying aquifer (Morin et al., 1988) is retarded with respect to the groundwater. Johnson et al. (2000) reported that the low pH plume of contaminated water at Nickel Rim

tailings impoundment moves at one tenth the average linear groundwater velocity.

The retardation at the Nordic Main tailings impoundment has been attributed to buffering of acidic waters by minerals present in the tailings and underlying aquifer (Dubrovsky et al., 1985; Morin et al., 1988). On the basis of field data, Morin et al. (1988) proposed a conceptual model of acid neutralization for the Elliot Lake uranium mill tailings. According to the conceptual model, the pH of the uranium tailings pore water is buffered by dissolution of a series of minerals (Fig. 1). The series consists of calcite, siderite, Al(OH)<sub>3</sub>, Fe(OH)<sub>3</sub>, and aluminosilicates. Blowes (1990) showed that the conceptual model of acid neutralization can be applied to explain the movement of acidic waters at three other sulfide-bearing mill tailings sites. Results of further field investigations of Coggans (1992) and Johnson (1993) are consistent with previous observations. The conceptual model was described in more detail by Blowes and Peacek (1994).

The conceptual acid neutralization model was proposed on the basis of field observations. Data collection points were widely distributed in space, and the groundwater flow pathways were assumed. Under laboratory conditions, it is possible to eliminate unknown influences that may have affected the geochemical evolution of the tailings pore water at the field sites. A laboratory column experiment was conducted to evaluate and refine the conceptual model and assess the mobility of metals in a detailed manner. Understanding acid neutralization in addition to acid generation processes is crucial in prediction, prevention, and remediation of environmental effects caused by the release of heavy metals. To evaluate the conceptual acid neutralization model and assess the mobility of metals, a laboratory column experiment was conducted using fresh, unoxi-

\* Author to whom correspondence should be addressed (jjurjove@uwaterloo.ca).

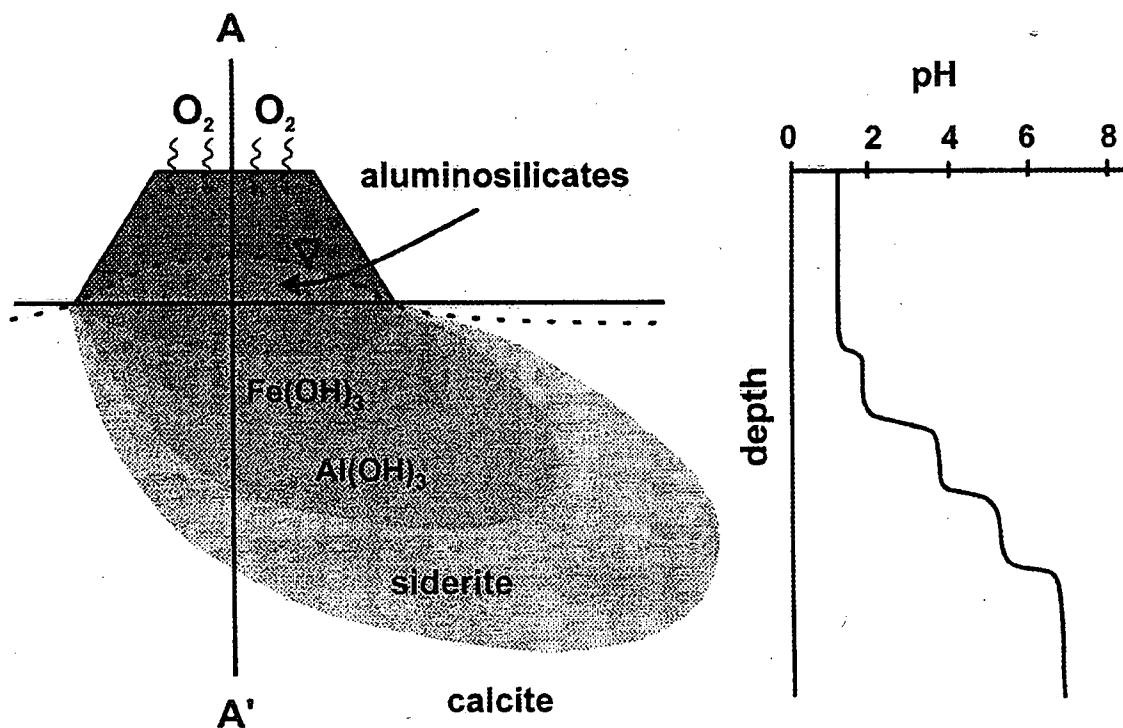


Fig. 1. Sketch of a tailings impoundment with a corresponding plume of acidic water and a diagram of pH changes with depth through cross-section AA'. Note: The vertical thickness of the plume is exaggerated.

dized tailings from the Kidd Creek metallurgical site. The measurements of the laboratory study are closely spaced in time; therefore, it is possible to discern the relative contributions of the pH buffering processes in far greater detail than is possible using field observations.

The second objective was to collect geochemical samples of the mill tailings pore water through time; a laboratory experiment permits collection of data temporally, providing a more precise description of changes in the pH and Eh and in the concentrations of dissolved metals. In the laboratory experiment, the acid neutralization process was followed from the beginning to completion. Because reactions in mine tailings sites occur slowly, the collection of field data at this level of temporal discrimination would be costly and impractical.

## 2. MATERIALS AND METHODS

### 2.1. Materials

#### 2.1.1. Solids

The solids used in the experiments were fresh, unoxidized tailings collected at the concentrator at the Kidd Creek metallurgical site near Timmins, Ontario. The mill tailings were oven dried at 100°C at the site. The mineralogy of the tailings sample was determined by Jambor et al. (1993) to be as follows: 15.1 wt.% sulfides, 8 wt.% carbonates and Fe-oxides, 49.1 wt.% quartz, and the balance of silicates and aluminosilicates. Information about identified minerals and mineral proportions in the tailings sample is summarized in Table 1.

In the same study, Jambor et al. (1993) investigated the composition of carbonates in the tailings samples from the Kidd Creek main impoundment. They identified the following carbonates using electron microprobe analyses and X-ray studies: calcite, dolomite, ankerite, and

siderite. These carbonates are rarely of the end-member composition. The average cation compositions for siderite and ankerite, as quantified through microprobe analysis, were found to be  $\text{Fe}_{0.904}\text{Mg}_{0.066}\text{Mn}_{0.022}\text{Ca}_{0.008}$  and  $\text{Fe}_{0.259}\text{Mg}_{0.210}\text{Mn}_{0.003}\text{Ca}_{0.499}$ , respectively. On the basis of the unadjusted diffraction intensities observed on the X-ray diffraction (XRD) patterns, the relative proportions of carbonates in the main impoundment were determined to be 5% calcite, 35% dolomite-ankerite, and 60% siderite. Because calcite is present in trace amount, it does not represent a significant control in this system. Therefore, the saturation indices for calcite have been omitted from the plots presented in this paper.

Following the experiment, the leached solid sample was divided into three parts: top, middle, and bottom. One sample was taken from each part. These three samples and two splits of starting material were analyzed by Activation Laboratories, Ltd., Ancaster, Ontario. Total S and CO<sub>2</sub> were analyzed using a LECO induction furnace. Si, Al, Fe<sub>tot</sub>, Mn, Mg, Ca, Na, K, Ti, and P were analyzed by inductively coupled argon plasma atomic emission spectrometry (ICP-AES) after a Li-metaborate fusion. Cu, Pb, Zn, Ni, and V were also measured by ICP-AES after a HNO<sub>3</sub>-HCl-HClO<sub>4</sub>-HF digestion. Co and Cr were determined by instrumental neutron activation analysis.

#### 2.1.2. Solutions

The synthetic background water was prepared by adding reagent-grade CaCO<sub>3</sub> and CaSO<sub>4</sub> to double-deionized water in excess of saturation. The solution was bubbled with CO<sub>2</sub> for 12 h to promote the dissolution of CaCO<sub>3</sub>. The solution was then equilibrated at atmospheric P<sub>CO2</sub> for 1 week. The tracer solution was prepared by adding reagent-grade NaCl to the synthetic background solution. The concentration of NaCl in the tracer solution was 0.1 mol/L. The experimental solution was prepared from ultrapure H<sub>2</sub>SO<sub>4</sub> and double-deionized water. The final solution was 0.105 mol/L H<sub>2</sub>SO<sub>4</sub>.

Table 1. Mineralogy of the tailings sample as obtained by image analysis study (Jamhor et al., 1993).

Mineral class	Mineral name	Formula	wt. %
Sulfides	Pyrite	$\text{FeS}_2$	13.2
	Pyrrhotite	$\text{Fe}_{1-x}\text{S}$	1.2
	Chalcocopyrite	$\text{CuFeS}_2$	0.5
	Sphalerite	$\text{ZnS}$	0.2
Silicates	Chlorite	$(\text{Mg}, \text{Fe})_3(\text{Si}, \text{Al})_4\text{O}_{10}(\text{OH})_2 \cdot (\text{Mg}, \text{Fe})_3(\text{OH})_6$	21.4
	Amphibole	$\text{W}_{0-1}\text{X}_2\text{Y}_3\text{Z}_6\text{O}_{22}(\text{OH}, \text{F})_2^a$	0.5
	Stiplnomelane	$\text{K}_{0.6}(\text{Mg}, \text{Fe}^{2+}, \text{Fe}^{3+})_6\text{Si}_8\text{Al}(\text{O}, \text{OH})_{27}2-4\text{H}_2\text{O}$	<0.5
	Albite	$\text{Na Al Si}_3\text{O}_8$	0.7
	Muscovite	$\text{KAl}_2(\text{AlSi}_3\text{O}_{10})(\text{OH})_2$	2.5
Carbonates <sup>c</sup> and Fe-oxides	Quartz	$\text{SiO}_2$	49.1
	Ankerite-dolomite	$\text{Ca}(\text{Fe}, \text{Mg})(\text{CO}_3)_2$	3.1
	Siderite and Fe-oxide	$\text{FeCO}_3, \text{Fe}_2\text{O}_3$	4.9
	gypsum	$\text{CaSO}_4 \cdot 2\text{H}_2\text{O}$	0.5

<sup>a</sup> Where W =  $\text{Na}^+/\text{K}^+$ ; X =  $\text{Ca}^{2+}, \text{Na}^+, \text{Mn}^{2+}, \text{Fe}^{2+}, \text{Mg}^{2+}, \text{Li}^+$ ; Y =  $\text{Mn}^{2+}, \text{Fe}^{2+}, \text{Mg}^{2+}, \text{Fe}^{3+}, \text{Al}^{3+}, \text{Tl}^{+}$ ; and Z =  $\text{Si}^{4+}, \text{Al}^{3+}$ .

<sup>b</sup> The minerals were undistinguishable by image analyses.

<sup>c</sup> For more detail on carbonates, see section 2.1.1.

## 2.2. Column Procedures

The experimental setup consisted of a reservoir, an Ismatic IP-4 peristaltic pump, a column, and a sampling cell (Fig. 2). Tailings were packed into a 10-cm-long clear acrylic column, 9.0 cm in internal diameter. No stratification of the tailings was observed after packing. The column was sealed with Viton O-rings. Nytex and Vycon (mesh size 30  $\mu\text{m}$ ) screens were used as filters to prevent flushing of the solids from the column. The screens were placed at the bottom and top column endplates. The Nytex screen was placed immediately on the tailings, followed by Vycon screen.

The column was first flushed with  $\text{CO}_2$  gas to displace air from the column (Pracek and Gillham, 1992). The column was then slowly saturated from bottom to top with synthetic background water. The synthetic background water was saturated with calcite and gypsum to prevent leaching of these two phases during the saturation of the column as well as during the tracer experiment to prevent changes in mineralogy before initiation of the experiment. The porosity of the tailings sample was determined to be 0.44 on the basis of the gravimetric measurements and CXTFIT modeling (Parker and van Genuchten, 1994). The water was passed through the column until a uniform flow rate was obtained. The flow rate was measured gravimetrically throughout the experiment. After establishing the uniform flow rate, a conservative tracer test was performed to determine flow and solute transport parameters using NaCl tracer solution. Water samples were collected every 30 min using a fraction collector for Cl determination.

The NaCl tracer solution was flushed out with the synthetic background water. During the acid neutralization experiment, the 0.105 mol/L  $\text{H}_2\text{SO}_4$  solution was passed through the column material for 150 pore volumes.

## 2.3. Sampling and Analytical Procedures

At the beginning of the experiment, during carbonate dissolution, a buildup of gas occurred in the sampling cell, preventing sufficient effluent water collection in the sampling cell. After initial testing, a sampling cell was designed to avoid trapping gas. The cell was constructed so that the inlet for the sample entered the cell from the bottom at an angle, and the outlet was at the top of the cell. This design allowed the gas ( $\text{CO}_2$ ) to pass through the cell and minimized mixing of the effluent water.

Samples of column effluent water were collected as a function of time. Effluent water samples were transferred from the sampling cell into a plastic syringe previously flushed with Ar gas. During sampling, the sampling cell outlet was connected to an Ar gas line to prevent  $\text{O}_2$  from entering into the sampling cell. Using this setup, neither the currently collected sample nor the following sample was exposed to atmospheric  $\text{O}_2$ .

Alkalinity, pH, and Eh were determined immediately after sample collection. The pH and Eh were measured in sealed cells. The cells for pH and Eh measurement were constructed by placing an electrode in a

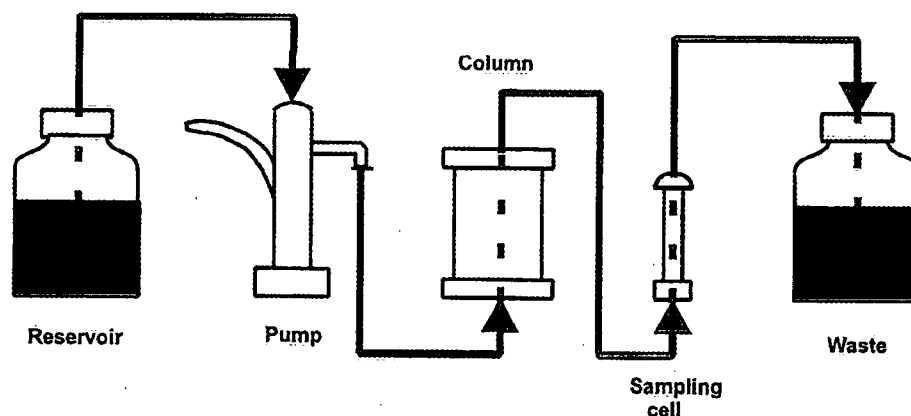


Fig. 2. Experimental setup.

5-mL syringe, which was sealed at the top by a Viton O-ring and Teflon cap and secured with a clamp to the syringe and electrode. Viton tubing was placed at the bottom of the syringe to allow for the transfer of the liquid sample from the sampling syringe to the cell for pH or Eh measurements. The pH was measured using a combination glass electrode (Orion Sure-Flow Ross 8165BN) calibrated with pH 4 and 7 standard buffer solutions and checked with pH 1.00 buffer solution (Fisher). The Eh was determined using a platinum combination electrode (Orion Model 9678BN), checked against ZoBell (Nordstrom, 1977) and Light solutions (Light, 1972). The Eh measurements were corrected to the standard hydrogen electrode. The samples were filtered through 0.45- $\mu$ m nylon filters. Alkalinity was determined by titration of filtered samples using a HACH digital titrator, indicator, and standardized sulfuric acid solutions. The indicator used to determine alkalinity was mixed bromocresol green-methyl red indicator solution (Greenberg et al., 1992). Samples, acidified to below pH 1, with trace metal hydrochloric acid were analyzed for cations. The samples for anions were not acidified. Because of the small size of the collected samples and rapid precipitation of solids from the unacidified samples, the  $\text{SO}_4$  analyses were not reproducible using unacidified samples. Therefore, we used acidified samples for  $\text{SO}_4$  analyses. No interference due to the presence of HCl was observed in the  $\text{SO}_4$  analyses.

Concentrations of Fe were determined colorimetrically using the Ferrozine method (Gibbs, 1979). Once a week, a fresh sample was analyzed with and without the addition of reductant, as suggested in the Gibbs (1979) procedure, to determine concentrations of total Fe concentrations and Fe(II). Thus, the concentration of Fe(III) was determined by the difference. The concentration of the Fe(II) was below the detection limit of the method throughout the experiment. Concentrations of  $\text{SO}_4$  were determined by ion chromatography and concentrations of Na, K, and Si by flame atomic absorption spectroscopy. The concentrations of Al, Ba, Be, Ca, Cd, Co, Cr, Cu, Li, Mg, Mn, Mo, Pb, Sr, V, and Zn were determined by inductively coupled plasma emission spectroscopy. The concentrations of Cl were determined colorimetrically using the ferricyanide method (Greenberg et al., 1992).

#### 2.4. Methods of Interpretation

Column flow and solute transport parameters were determined by modeling Cl concentrations measured during the tracer test and by gravimetrically measuring flow rate. The modeled parameters were obtained from the leading edges of the breakthrough curves using the nonlinear least squares optimization software CXTFIT (Parker and van Genuchten, 1994).

The pore water geochemistry was interpreted with the assistance of the equilibrium geochemical speciation/mass transfer model MINT-EQA2 (Allison et al., 1990). The thermodynamic database was adopted from the speciation model WATEQ4F (Ball and Nordstrom, 1991). Solubility data for siderite (Nordstrom et al., 1990; Ptacek, 1992),  $\text{FeH}_2\text{SiO}_4$  (Reardon, 1970), ankerite-dolomite (Al, 1996), and cobalt species (Papelis et al., 1988) were added. The degree of saturation of a mineral with respect to the solution in contact with the mineral in this paper is expressed as saturation index (SI). The SI is equal to the difference of logarithms of ion activity product and solubility constant:  $(\text{SI} = \log IAP - \log K_{sp})$ . An SI value of zero indicates equilibrium, a negative value undersaturation, and a positive value supersaturation. To ease comparison of SIs of minerals of widely different stoichiometries, the SIs were normalized according to the equation (Folmy and Weare, 1986)

$$\text{SI}_N = \frac{\left( \log \frac{IAP}{K} \right)}{N} \quad (1)$$

where  $IAP$  is the ion activity product,  $K$  is the equilibrium constant, and  $N$  is the number of ions in the solid phase.

### 3. RESULTS AND DISCUSSION

A column experiment was conducted with fresh unamended tailings from the Kidd Creek metallurgical site near Timmins, Ontario. At the Kidd Creek site, tailings are currently codis-

posed with natrojarosite, a waste product from the zinc refining process. This study focused on acid neutralization mechanisms and their effects on metal mobility within unamended tailings. A 0.105 mol/L sulfuric acid was passed through the column continuously. This solution was chosen to represent an approximation of acidic pore water generated in a generic unsaturated zone of a tailings impoundment. In the field situation, this solution eventually reaches the saturated zone; the zone simulated in the experiments. Pore waters of pH < 1 have been observed at tailings impoundments where tailings have been exposed to atmospheric conditions for longer periods of time. Examples of such impoundments are Heath Steele in central New Brunswick (Blowes et al., 1991), and Sherridon near Flin Flon, Manitoba (Ptacek et al., 2001). Moreover, negative-pH water has been observed at Iron Mountain, California (Nordstrom et al., 2000). Very low-pH pore waters have not been observed at the Kidd Creek metallurgical site. Tailings are currently being deposited at this site, and therefore, the tailings have not been exposed to weathering conditions for an extended time. The reason for selecting the 0.105-mol/L  $\text{H}_2\text{SO}_4$  solution was practical: to complete the experiment in a reasonable time (8 months). The measured pH of this sulfuric acid solution was  $0.95 \pm 0.6$ . Reactive transport simulations were conducted before the start of the experiment. The results of preliminary simulations conducted before the initiation of the experiments suggested that an input solution of pH 2 would result in a 10-fold increase in the duration of the experiment.

The calculated specific discharge used in this experiment was 0.33 cm/h, which translates to an average linear velocity of ~30 m/a. Average linear groundwater velocities reported for various tailings impoundments vary from 1 to 18 m/a (Blowes, 1990). The porosity of the tailings used in the column experiment was 0.44, which is consistent with what is observed in the field (Al, 1996).

#### 3.1. Measured Parameters in the Column Effluent Water as a Function of Pore Water (Figs. 4 and 5)

Measurements of effluent water pH during the experiment form a staircase-shaped curve (Fig. 3). There are three long plateaus at pH 5.7, 4.0, and 1.3. This observation is consistent with field observations of Dubrovsky (1986), Blowes (1990), Coggans (1992), and Johnson et al. (2000). The pH decreases abruptly from one plateau to another, with the change occurring over a few pore volumes.

Figure 5 shows that saturation indices for various carbonate minerals form plateaus, which correspond to the first pH plateau. At this time, alkalinity in the effluent water is high (around 500 mg/L; Fig. 3). These results suggest that the first pH plateau (pH = 5.7) occurs because of the presence of carbonates in the tailings.

Calculations based on the assumption that the solubility product of the dolomite-ankerite solid solution can be defined according to the observed stoichiometry suggest that the effluent water is slightly undersaturated with respect to ankerite-dolomite solid solution. This observation suggests that the dissolution of this mineral is kinetically limited. According to the acid neutralization model, the dissolution of carbonates and hydroxides are equilibrium reactions under field conditions. However, Al (1996) did not observe equilibrium of pore waters



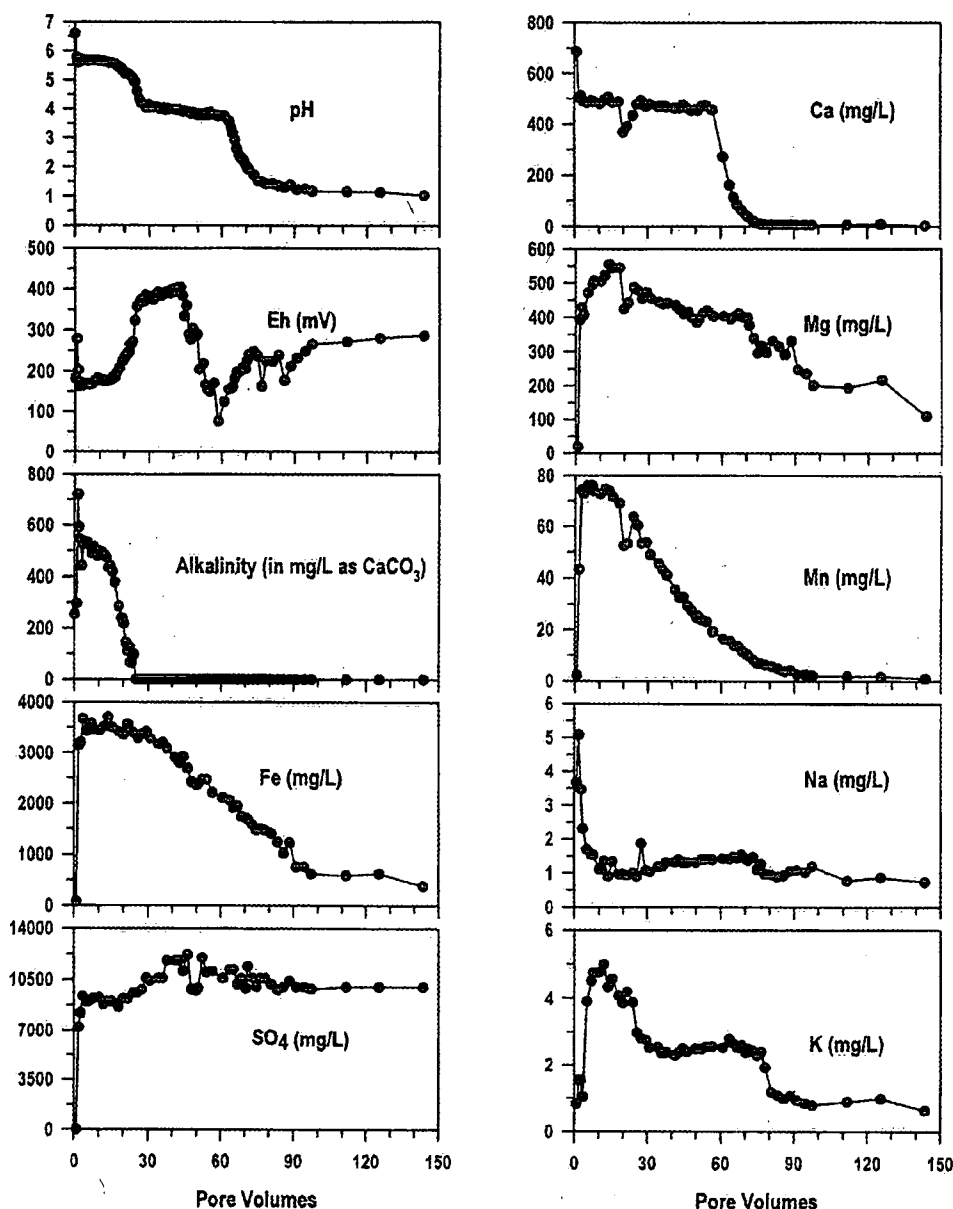


Fig. 3. Measured parameters in the column effluent water as a function of pore volumes.

at the Kidd Creek impoundment with respect to ankerite-dolomite solid solution. More recent observations by Al et al. (2000) indicated that the dissolution of carbonates in tailings impoundments is incongruent, which is inconsistent with the assumption of congruent dissolution used in equilibrium calculations.

Undersaturation of effluent water with respect to ankerite-dolomite solid solution suggests kinetically limited dissolution. Kinetically limited dissolution of an ankerite-dolomite solid solution is possible because of two factors: flow rate and precipitation of secondary minerals. The first factor, the flow rate of pore water through the column as well as in Kidd Creek tailings impoundment, may not allow sufficient time for the

reaction to reach equilibrium. The second factor, precipitation of secondary minerals, can result in mineral coatings that reduce the rate of mineral dissolution. Coatings of secondary gypsum on polished calcite crystals, which "passivated the surface against further reaction and dissolution," were observed by Booth et al. (1997). In their experiments, in which calcite was passed in a flow-through reactor and flushed with 0.1 mol/L  $\text{H}_2\text{SO}_4$ , a significant decrease in the dissolution rate of calcite was observed in <17 min.

The geochemical modeling of the effluent water from the column experiment indicates equilibrium with respect to gypsum during the first 60 pore volumes of the experiment. The results of the calculations are consistent with suggestion that

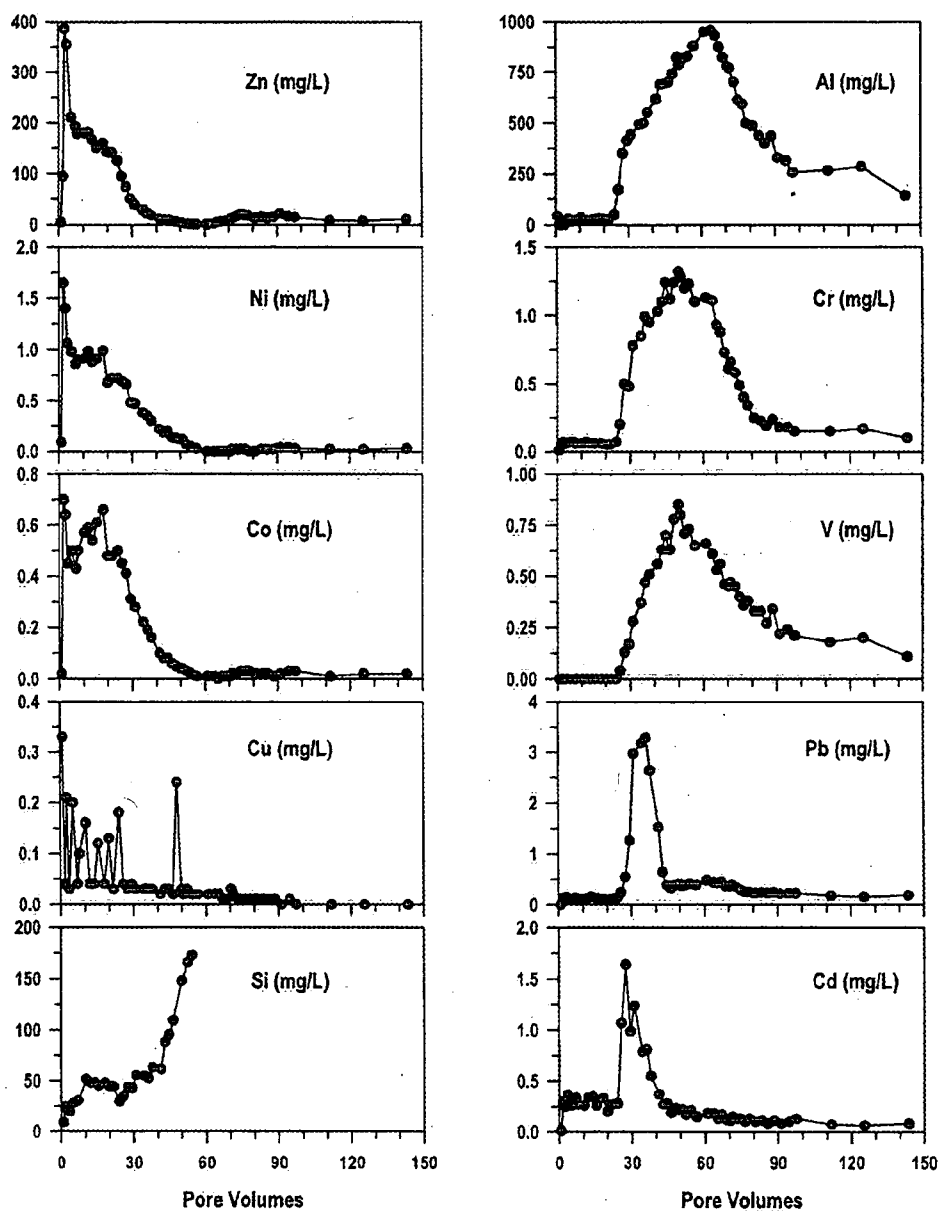


Fig. 4. Measured parameters in the column effluent water as a function of pore volumes.

the formation of gypsum coatings could lead to a decrease in the rate of ankerite-dolomite dissolution. The possibility of secondary mineral coatings reducing the rate of ankerite-dolomite solid solution is also supported by observations of Al et al. (2000). In their investigation of carbonate-mineral grains from five different geochemical zones at Kidd Creek tailings impoundment, Al et al. (2000) identified coatings of secondary siderite surrounding primary grains composed of the ankerite-dolomite solid solution.

At the first pH plateau, the effluent water is supersaturated with respect to siderite, suggesting formation of secondary siderite, which is consistent with the acid neutraliza-

tion model (Morin et al., 1988; Blowes and Ptacek, 1994) and with observation of secondary siderite by Al et al. (2000).

Field observations indicate two pH zones attributed to carbonate dissolution; the first zone is attributed to calcite, and the second is attributed to siderite. In this experiment, only one pH plateau, which could be attributed to carbonate-mineral dissolution, could be discerned. There are two reasons for the development of only one plateau. The first reason is that Kidd Creek tailings contain only a trace amount of calcite (section 2.1.1), which is not present in sufficient quantities to buffer the tailings pore water to the pH observed at other sites. Second,

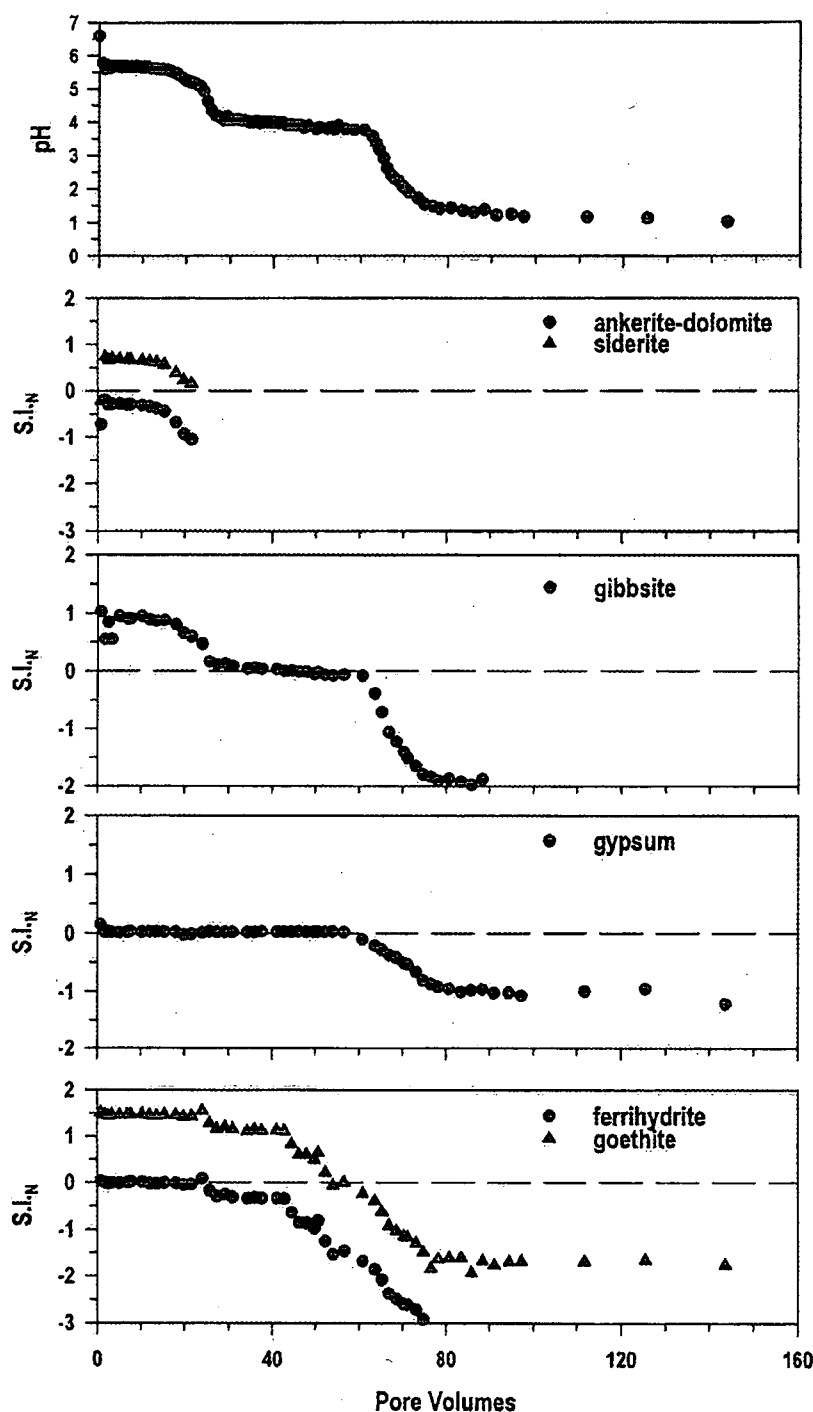


Fig. 5. Normalized saturation indices (S.I.N) of effluent water samples vs. pore volumes.

even though two carbonate minerals, the ankerite-dolomite solid solution and siderite, are present in the tailings in significant quantities (section 2.1.1 and Table 1), the measurements of pH and alkalinity indicate no significant difference in buffering potentials of these two minerals. Because Mg, Mn, and Ca substitute 10% of Fe in the Kidd Creek siderite, the siderite

present at Kidd Creek is more soluble than pure siderite. The smaller difference in solubility products of the two minerals may mask any difference in buffering potential. The first pH plateau, attributed to carbonate dissolution, is slightly sloped. On the basis of the observations of Al et al. (2000) and solid solution theory, the components of the most soluble end-mem-

ber will preferentially dissolve first, leaving behind the components of the less soluble end-member of a solid solution. Thus, the observed sloped pH plateau may indicate incongruent dissolution in a manner that is consistent with the field observations of Al et al. (2000). Results of the geochemical modeling suggest that as soon as ankerite-dolomite and siderite are depleted, the pH of the effluent decreases abruptly. Depletion of alkalinity coinciding with the first abrupt pH decrease is consistent with this conclusion (Fig. 3). XRD patterns of a solid sample collected after the completion of the experiment show no indication of the presence of carbonates. These observations are consistent with field observations at Nickel Rim mine tailings impoundment, where an order of magnitude decrease in carbonate content in tailings was observed in solid samples where the pore water pH decreased below 4.5 (Johnson et al., 2000). Sampling of solids in the column during this experiment was not possible without significantly disturbing the flow of pore water.

During the first pH plateau region, the effluent water is near equilibrium with respect to ferrihydrite. At the same time, the effluent water is supersaturated with respect to gibbsite and goethite, indicating a tendency for precipitation of these minerals at the beginning of the experiment, when the pH is still high (Fig. 5). This observation is consistent with field observations of Blowes (1990) and Johnson et al. (2000).

At the second pH plateau, which occurs at pH 4.0, the effluent water is in equilibrium with respect to gibbsite (Fig. 5). The second pH plateau occurs from 25 to 61 pore volumes. At this time, Al concentrations steadily increase from <10 to 1000 mg/L. A sudden decrease in Al concentrations at 60 pore volumes coincides with the second abrupt decrease in measured pH (Figs. 3 and 5). At the same time, the effluent water becomes undersaturated with respect to gibbsite and boehmite, suggesting that the mass of these two minerals is not sufficient to buffer the acidic solution passing through the column. This observation is consistent with field observations in a series of tailings impoundments (Dubrovsky et al., 1985; Blowes and Jambor, 1990; Johnson et al., 2000). However, neither primary nor secondary gibbsite have yet been identified in a tailings environment. It is possible that the mass of gibbsite is too small to be detected easily with the mineralogical techniques used, or another mineral that exhibits a dissolution solubility product similar to gibbsite controls the pH of pore water at the second plateau.

During the first portion of the second pH plateau, the effluent water is slightly undersaturated with respect to ferrihydrite, which suggests near equilibrium dissolution of ferrihydrite. Small amounts of primary iron oxyhydroxides have been observed in the tailings. An abrupt decrease in ferrihydrite saturation indices at 42 pore volumes suggests depletion of ferrihydrite from the column before the pore water pH decreases to the third plateau. This observation suggests that it is unlikely that ferrihydrite would be the pH-controlling phase of the second plateau. The observation is inconsistent with the field observations of Dubrovsky (1986), Blowes (1990), and Johnson et al. (2000), which suggest that ferrihydrite is the dominant buffer at pH 2.8 to 3.0. A likely reason for the absence of this plateau in this experiment is that the tailings used in the experiment were fresh and unoxidized. The mass of primary oxyhydroxides was likely too small and was depleted before

these minerals could become the primary pH buffer in the tailings. Because the experiment was conducted to observe acid neutralization reaction in isolation from acid-producing reactions, secondary ferrihydrite did not precipitate in sufficient quantities to buffer the pore water pH. This conclusion is supported by measurements of Fe(II) in the effluent water. The difference between the  $Fe_{tot}$  and Fe(II) was not discernable throughout the experiment.

The last pH-plateau develops at pH 1.3, when the pore water pH is likely controlled by kinetic dissolution of aluminosilicate minerals. This interpretation is supported with the presence of high concentrations of Al and Si in the effluent water. Observations from similar experiments on Kidd Creek tailings suggest that Si concentrations in the pore water remain high until the end of the experiment (unpublished data).

### 3.1.1. Major Ions

The concentration of Ca decreases at the beginning of the experiment from ~700 to 500 mg/L and remains constant until 59 pore volumes (Fig. 5). The only exception is a short, abrupt decrease in Ca concentrations at 20 pore volumes when Ca concentrations decrease to 350 mg/L. The abrupt decrease in Ca concentrations corresponds to a decrease in alkalinity, which coincides with the depletion of carbonate from the column material. Similar decreases in concentration in effluent water samples at 20 pore volumes were observed for Mg, Mn, Co, and Ni. The water samples were reanalyzed for Ca using a different analytical technique to confirm the analyses.

The high Ca concentrations persist because of dissolution of the following minerals: ankerite-dolomite solid solution, gypsum, and minor substitutions in siderite. Results of geochemical modeling indicate that Ca concentrations are controlled by gypsum dissolution from the beginning of the experiment until 59 pore volumes, when the effluent water becomes undersaturated with respect to gypsum. This observation suggests depletion of gypsum from the column. The decrease in Ca concentrations is abrupt; Ca concentrations decrease from 500 to below 10 mg/L over 15 pore volumes (Fig. 3.).

The concentrations of Mg increase abruptly to ~400 mg/L during the first pore volume of the experiment. During the next 20 pore volumes, the concentration of Mg slowly increases from 400 to 550 mg/L, which may indicate incongruent dissolution of carbonate minerals. Mg concentrations start to decrease at the same time as the alkalinity decreases abruptly. In contrast to alkalinity, Mg concentrations decrease gradually through the entire experiment to 100 mg/L (Fig. 3). Minerals present in the tailings, which contain Mg, are the ankerite-dolomite solid solution, chlorite, amphibole, stilpnomelane, and talc. The largest amount of Mg is contained in chlorite (Table 1). The sources of Mg are mainly ankerite-dolomite and chlorite because of their abundance and solubility. After the first abrupt pH decline and depletion of alkalinity, the majority of the Mg is probably derived from the dissolution of chlorite. This hypothesis is supported by XRD patterns, which indicate 60 wt.% chlorite depletion from the initial material over the course of the experiment (Jambor, 2000, personal communication). This observation is consistent with field observations at the Heath Steele tailings impoundment (Blowes, 1990). Minor amounts of Mg may come from stilpnomelane.

The shape of the Fe concentration curve for the effluent water is very similar to the shape observed for Mg. The only difference is that Fe concentrations are significantly higher than those of Mg. This observation suggests that the major sources of these two ions are similar. The Fe concentration increases abruptly at the very beginning of the experiment, to 3500 mg/L, and then gradually decreases to 800 mg/L at 95 pore volumes. Thereafter, Fe concentrations in the effluent water remain constant at approximately 800 mg/L until the end of the experiment. The beginning of the gradual decrease corresponds to the decrease in Mg concentration, alkalinity, and pH, which suggests that carbonate minerals are a significant source of dissolved iron. After the first abrupt decrease in pH, the main source of the elevated Fe concentrations is chlorite. Other potential sources of Fe are stilpnomelane, Fe-oxyhydroxides, and sulfides. The amounts of stilpnomelane and Fe-oxyhydroxides are too small to account for the mass of Fe observed (Table 1).

The solids at the end of the experiment (i.e., leached material samples) were collected to determine the changes in mineralogy. The column solids were divided in three sections from top to bottom. XRD analyses of the leached samples indicate that 50% of the chlorite present in the starting material was depleted during the experiment (J. L. Jambor, 2000, personal communication). The results of XRD analyses indicate the absence of carbonates in the leached samples (Jambor et al., 1993). The results of XRD analyses are consistent with chemical analyses of the solid samples. This observation supports the hypothesis that chlorite is a major contributor of Fe concentrations in the pore water.

Concentrations of  $\text{SO}_4$  increase up to 9500 mg/L in the first two pore volumes after the initiation of the experiment. After 30 pore volumes, the concentrations of  $\text{SO}_4$  increase to ~11,000 mg/L and then slowly decrease to ~10,000 mg/L (Fig. 3). The concentrations of  $\text{SO}_4$  remain lower during the first 25 pore volumes when alkalinity is high. Lower concentrations of  $\text{SO}_4$  are due to dissolution of carbonates providing Ca. Therefore, gypsum precipitation likely occurred at the beginning of the experiment. As the carbonate minerals are depleted,  $\text{SO}_4$  concentrations increase. The results of geochemical modeling indicate that gypsum dissolution and reprecipitation is an equilibrium reaction during the first 60 pore volumes, which further suggests that  $\text{SO}_4$  concentrations are limited by gypsum solubility at this time (Fig. 5). This hypothesis is also supported by identification of gypsum in the tailings (Table 1).

The Al concentrations are low (20 to 30 mg/L) during the first 25 pore volumes. During this time, pH is still high. After 30 pore volumes, Al concentrations increase steadily to 960 mg/L until 74 pore volumes. After achieving maximum values, Al concentrations start to decrease until 92 pore volumes and remain constant at 250 mg/L for the rest of the experiment (Fig. 4). The increase in Al concentrations corresponds to the depletion in alkalinity, increase in Eh, and abrupt decrease in pH. Results of geochemical modeling indicate that gibbsite precipitation is favored during the first 30 pore volumes (Fig. 5). The source of Al is aluminosilicate dissolution, namely, dissolution of chlorite. Further, results of geochemical modeling suggest that pore water is in equilibrium with respect to gibbsite at the second plateau. This suggests that Al concentrations are limited

by gibbsite solubility from 25 to 62 pore volumes. After 62 pore volumes, Al concentrations abruptly decrease, which is consistent with undersaturation of gibbsite with respect to the effluent water. Only minor amounts of aluminum are expected to be derived from dissolution of muscovite and stilpnomelane because of their low abundance in Kidd Creek tailings. On the basis of increased rates of aluminosilicate dissolution at lower pH, additional sources of Al at the third pH plateau may be albite and amphibole.

The shape of Mn curve vs. time is similar to that of Mg. However, concentrations of Mn in the effluent water are about one tenth the concentrations of Mg, with the highest concentrations just over 70 mg/L. After 25 pore volumes, the Mn concentrations decrease more rapidly than the Mg concentrations, suggesting that Mn is depleted more slowly or that the source of Mg is depleted preferentially over Mn (different ratios). Minor amounts of Mn were identified in both carbonates present in the Kidd Creek tailings (section 2.1.1). Microprobe analyses of chlorite from the Kidd Creek deposit detected Mn as a minor component. Other possible sources of Mn could be substitutions in other aluminosilicates present in the Kidd Creek tailings.

The concentrations of Na decrease from 5 to ~1 mg/L and remain low throughout the experiment (Fig. 3). The only encountered mineral containing Na is albite.

The shape of K concentrations is similar to the shape of the pH curve (Fig. 3). The concentrations of K increase slightly at the beginning of the experiment, reaching peak concentrations at around 10 pore volumes. The concentrations of K decrease abruptly in two steps. The first decrease corresponds to the first decrease in pH, depletion in alkalinity, and abrupt increase in aluminum concentrations. The second decrease in K concentrations occurs just after Al concentrations become constant. The only two encountered sources of K in the tailings are muscovite and stilpnomelane, which are both likely to dissolve.

### 3.2. Metal Mobility

The results of this column experiment represent a detailed temporal observation of pH, Eh, and metal concentrations in tailings and confirm that metal mobility depends on pH. The results indicate that the metals can be divided into three groups on the basis of their mobility. Zn, Ni, and Co become mobile at the beginning of the experiment, as soon as the pH of the pore water decreases to 5.7. Cadmium, Cr, V, and Pb become mobile when pH decreases to 4.0, whereas Cu concentrations remain unaffected by changes in pH. This observation indicates that Zn, Ni, and Co are more mobile in moderately acidic pore waters than Cd, Cr, V, and Pb. This observation is similar to the field observations reported by Blowes and Jambor (1990), who observed the following general order of metal mobility at the Waite Amulet tailings site:  $\text{Zn} > \text{Ni} \approx \text{Co} > \text{Pb} > \text{Cu}$ . The results of our experiment are also in agreement with the order reported by Dubrovsky (1986) at the Nordic Main tailings impoundment near Elliot Lake, Ontario, where metal mobility was  $\text{Co} = \text{Ni} > \text{Zn} > \text{Pb} > \text{Cu}$ .

Total elemental concentrations of leached samples indicate that most of the metal mass remains in the solid sample and was not leached during the experiment, suggesting that metals in

Kidd Creek tailings must be present in at least two forms. MINTEQA2 calculations suggest that Fe(III)-(oxy)hydroxides dissolved during the experiment. Ribet et al. (1995) determined in their experiments that >80% of Fe, Ni, Cu, Cr, and Co in Nickel Rim oxidized tailings are associated with the reducible fraction that is mainly composed of Fe(III)-(oxy)hydroxides. This provides an indication that Fe(III)-(oxy)hydroxides may be the source of the metals leached during the experiment. Given that our experiments were performed with relatively unoxidized tailings with a very small content of Fe(III)-(oxy)hydroxides (Table 1), most of the metals that remained in the leached sample were in the sulfide form, as Cu, As, Pb and Zn sulfide minerals were identified in Kidd Creek tailings (Jambor et al., 1993).

The concentrations of metals in pore water depend on pH, the amount of Fe(III)-(oxy)hydroxide present in the tailings, and on the amount of metals sorbed on the Fe(III)-(oxy)hydroxide surface. At the Kidd Creek concentrator, lime is added to the tailings before discharge. A tailings sample collected from the thickener before discharge indicated a pH of 6.88 (Tom A. Al, 2001, personal communication). Sorption experiments reported by Stumm and Morgan (1996) indicate that at pH 5.7, all adsorbed Zn, almost all of the adsorbed Ni, Cd, and 20% of Cu were released. Cr and Pb, on the other hand, remain bound. If the tailings contained different carbonates with different buffering capacities, pH plateaus might appear at different pH values, which would in turn imply different ratios of released metals. Moreover, larger amounts of metals bound to the Fe(III)-(oxy)hydroxide surface would result in a larger mass of metals at the same pH levels.

### 3.2.1. The First Group of Metals

**3.2.1.1. Zn.** Among all the metals, Zn reaches the highest concentrations (Fig. 4). At the beginning of the experiment, the concentration increases to almost 400 mg/L and sharply decreases thereafter until 60 pore volumes, when it decreases below 10 mg/L. Measurements of adsorption of Zn on the surfaces of hydrous ferric oxide (HFO) suggest that the tendency for Zn adsorption decreases as the pH decreases (Dzombak and Morel, 1990), with extensive adsorption occurring at pH > 6 and little Zn adsorption at pH < 4. Kinniburgh et al. (1976) defined the  $pH_{50}$  as an indicator of the relative affinity of metals for the mineral surface. The  $pH_{50}$  is defined as the pH at which 50% of the cation in solution is adsorbed. Kinniburgh et al. (1976) observed that for fresh iron hydroxide gel, the  $pH_{50}$  was 5.4. The sharp increase in Zn concentrations to 400 mg/L occurs in the earliest stage of the experiment as the pH decreases from 6.6 to 5.7; this is followed by a more gradual decline as the pH falls from 5.7 to <5.0. The subsequent decrease in Zn concentration to below 10 mg/L corresponds to a decrease of saturation indices for ferrihydrite to <0, also observed at 60 pore volumes. These observations suggest that high concentrations of Zn are released by desorption from ferrihydrite, or dissolution of ferrihydrite and release of coprecipitated Zn from within the ferrihydrite structure. Dissolution of ferrihydrite and/or other ferric oxyhydroxides was observed visually during the experiment. The dissolution front moved from the bottom to the top of the column. The flow direction was from the bottom to the top of the column. The concentra-

tion of Zn increases slightly as soon as pH decreases below 2. From 70 pore volumes on, Zn is probably derived from dissolution of sphalerite, which was identified in the Kidd Creek tailings (Jambor et al., 1993). These results indicate that Zn is mobile under intermediate-pH conditions that can be maintained by buffering reactions due to dissolution of minerals present in the Kidd Creek tailings.

**3.2.1.1. Ni.** The shape of the plot of Ni concentrations vs. pore volumes is very similar to the shape of Zn concentrations (Fig. 4). However, the concentrations are 2 orders of magnitude lower, with the highest Ni concentration of 1.65 mg/L observed at the beginning of the experiment. Similar to Zn, the concentration of Ni decreases below its detection limit of 0.02 mg/L at 60 pore volumes. Dzombak and Morel (1990) observed that 25% of Ni adsorbed to HFO surface at pH 6.6. These observations suggest that Ni in the column effluent water is likely derived by release of Ni contained in ferrihydrite or other ferric oxyhydroxide minerals present in the tailings or by desorption from ferric oxyhydroxides when the pore water pH declines by the introduction of low-pH input solution. No primary or secondary Ni phase was encountered by Jambor et al. (1993) in their mineralogical study of the Kidd Creek tailings. However, Ni was found to substitute in various sulfides (Thorpe et al., 1976). The chemical analyses of leached solid samples indicate that 43 ppm Ni remains in the tailings after the completion of the experiment.

**3.2.1.3. Co.** The geochemical behavior of Co is very similar to Ni and Zn (Fig. 4). However, the concentrations are the lowest among all of the three metals. The highest concentration of Co reaches 0.7 mg/L and decreases close to its detection limit of 0.01 mg/L at 60 pore volumes. The similarity of the shape of the Co curve to that of Zn and Ni and agreement with the ferrihydrite depletion suggest the same source of Co. This hypothesis is consistent with the observations of Dzombak and Morel (1990), who observed that at pH 6.6, 30% of Co contained in their experimental system was adsorbed to the HFO surface. Cobalt contained in the effluent water can be derived from within the ferric oxyhydroxide structure or released from its surface when the chemistry of pore water changes. Again, the analyses of solid samples suggest that most of the Co is not leached out during the experiment.

### 3.2.2. The Second Group of Metals

The second group of elements (Pb, Cr, Cd, and V) shows similar geochemical behavior in effluent water concentrations. The concentrations of all these elements were very low during the first 25 pore volumes, while pH is 5.7, after which concentrations of all four elements increase abruptly as soon as the pH drops to the second plateau (pH = 4.0) and Eh increases from 160 to 400 mV.

**3.2.2.1. Pb.** The concentrations of Pb remain below 0.15 mg/L during the first 25 pore volumes when pH is high (pH = 5.7). As the pH decreases abruptly from 5.7 to 4.0, Eh increases and alkalinity is depleted, and the concentration of Pb increases sharply to 3 mg/L (Fig. 4). The abrupt decrease in Pb concentrations corresponds to the decrease in the ferrihydrite saturation indices, which suggests that Pb is either adsorbed to and/or coprecipitated with ferrihydrite (Fig. 4). After 40 pore volumes, the concentration of Pb remains below 0.5 mg/L.

The results of sorption experiments reported by Dzombak and Morel (1990) indicate the tendency for extensive adsorption of Pb occurring at pH > 5.5 and little Pb adsorption at pH < 3. The comparison of our results with the results of sorption experiments by Dzombak and Morel (1990) indicates that the majority of Pb at pH 5.7 is adsorbed by ferrihydrite. When pH decreases to 4.0, 80% of the Pb is reported to be in solution (Dzombak and Morel, 1990; Stumm and Morgan, 1996). These results suggest that the source of Pb is ferrihydrite or other ferric oxyhydroxides. MINTEQA2 modeling suggests that effluent pore water samples between 30 and 40 pore volumes, where Pb concentrations reach peak, are in equilibrium with respect to anglesite (not shown). This observation suggests a tendency for anglesite precipitation between 30 and 40 pore volumes and thus a possible control of Pb concentrations between 30 and 40 pore volumes. No anglesite was encountered in the fresh tailings sample during mineralogical investigation (Jambor et al., 1993). The only encountered source of Pb in the fresh Kidd Creek tailings is galena (Jambor et al., 1993). Corroded edges of galena identified during mineralogical investigation suggest that the low Pb concentrations at the end of the experiment when pH decreases to 1.3 are derived from galena dissolution.

**3.2.2.2. Cd.** The concentrations of Cd are around 0.25 mg/L at the first pH plateau. The concentrations increase abruptly as pH decreases to 4.0 and Eh increases to 400 mV. Similar to Pb, Cd concentrations decrease as soon as Eh decreases. After 40 pore volumes Cd concentrations remain low, below 0.2 mg/L. No source of cadmium was encountered in the tailings. However, TOF-LIMS analyses show high concentrations of Cd on the surface of siderite grains collected from the Kidd Creek tailings impoundment (Al et al., 2000). Low concentrations during the first 25 pore volumes and abrupt increase in Cd concentrations at pH 4 suggest that Cd concentrations in the effluent pore water are controlled by adsorption and desorption processes on carbonates surfaces. That is, Cd concentrations remain low as long as carbonates are present. Upon the depletion of carbonates from the column, the Cd concentration abruptly declines because of depletion of the controlling phase. Observations of previous researchers suggest that trace Cd concentrations in pore water are likely controlled by adsorption to calcite surfaces (Fuller and Davis 1987; Davis et al., 1987; Supp et al., 1992).

An average 0.30 wt.% of Cd has been identified by microprobe analyses of Kidd Creek sphalerite grains (Dutrizaq and Chen, 1990). However, the calculations show that the ratio of Cd/Zn in effluent water samples from the column is from 1 to 2 orders of magnitude lower than that observed in the sphalerite, except for two water samples.

**3.2.2.3. V and Cr.** At 25 pore volumes, the concentration of V increases abruptly to 0.85 mg/L. Although the concentration jump occurs at the same time as the jump in concentrations of Pb and Cd, we believe that dissolution of V is controlled by a different mechanism than the dissolution of Pb and Cr. Namely, the high concentrations of V persist beyond the point of ferrihydrite depletion. The curve for V is, however, of a similar shape as the curve for Al. This suggests an aluminum-bearing mineral as a source of V, which is supported by the observation that V is frequently associated with sheet silicates (Jambor et al., 1993). The Cr curve is of a similar shape as the curves for

V and Al. This may be an indication that the source of Cr is the same as or similar to the source of V.

### 3.2.3. The Third Group of Metals

**3.2.3.1. Cu.** The concentrations of Cu are unaffected by pH changes during the experiment and remain close to the detection limit of 0.01 mg/L throughout the experiment (Fig. 4). Chemical analysis of a solid sample leached in the experiment show that Cu was still present in the column materials after the experiment was completed. Secondary covellite was observed in polished thin sections of leached solid samples by mineralogical analyses (J. L. Jambor, 1999, personal communication). A number of sulfides containing Cu were identified in the Kidd Creek tailings: chalcopyrite, tennantite, tetrahedrite, and bornite. Formation of secondary covellite was inferred to control aqueous Cu concentrations in the Heath Steele tailings impoundment (Boorman and Watson, 1976). Secondary covellite has also been observed at the Waite Amulet tailings impoundment (Blowes and Jambor, 1990) and at the Nickel Rim tailings impoundment (Johnson et al., 2000).

## 4. CONCLUSIONS

To evaluate and refine a conceptual acid neutralization model and assess the mobility of metals in a detailed manner, a laboratory column experiment was conducted using fresh, unamended Kidd Creek tailings. This column procedure enables the study of acid neutralization mechanisms in tailings and enables the estimation of arrival times for various metals. The results of this experiment represent a temporal observation of changes in pH, Eh, and metal concentrations. The experimental results are consistent with the proposed conceptual model of Morin et al. (1988).

For the fresh, unamended Kidd Creek tailings, the results of geochemical modeling indicate that ankerite-dolomite, siderite, gibbsite, and aluminosilicates control the pH of the effluent water. In the column study, no significant difference was discerned in the buffering ability of ankerite-dolomite and primary siderite. In this experiment, ferrihydrite is not the primary control of the pore water pH, as suggested by Morin and Cherry (1986) and observed by Blowes (1990). The absence of ferrihydrite as a buffering phase in this study is attributed to the use of unoxidized tailings. Had the tailings been allowed to oxidize, ferrihydrite would be an abundant secondary precipitate in the unsaturated zone, derived from early periods of oxidation, when carbonates act as the primary buffer (Blowes and Ptacek, 1994) and would thus control the pH of pore water.

Measured metal concentrations indicate that metal mobility in the effluent water is controlled by the pH. The metals can be divided into three groups on the basis of their mobility. Zinc, Ni, and Co become mobile at pH 5.7, and Cr, V, Pb, and Cd become mobile at pH 4.0. Cu concentrations remain unaffected by pH changes. The source of Zn, Ni, Co, Pb, and Cd is Fe(III)-(oxy)hydroxide, while V and Cr originate from a different source, probably aluminosilicates. Because the experiment was performed with fresh, unoxidized tailings that contain only a small amount of Fe(III)-(oxy)hydroxide, concentrations of leached metals persisted for a relatively short period of time.

In a field situation, where tailings can oxidize, there is a potential for significantly higher amounts of leached metals.

**Acknowledgments**—The authors would like to thank John Jambor for conducting the mineralogical analyses of the Kidd Creek tailings, which greatly improved this paper. The authors would like to thank Rhonda Wojto and Lia Hinch of the University of Waterloo for their assistance with the experimental work. The Ontario Ministry of Colleges and Universities provided the funding for this research through the University Research Initiative Fund. Environment Canada of Burlington, Ontario, provided funding for laboratory analyses of water samples by ICP. In addition, the Canadian Natural Science and Engineering Research Council supported this study through research grants provided to Carol J. Ptacek and David W. Blowes. The Ontario Ministry of Colleges and Universities provided graduate scholarship support to the first author. The authors would also like to thank R. Seale and an anonymous reviewer for their constructive comments.


Associate editor: J. D. Rimstidt

## REFERENCES

- Al T. A. (1996) *The Hydrology and Geochemistry of Thickened, Sulfide-Rich Tailings, Kidd Creek Mine, Timmins, Ontario*. Ph.D. thesis, University of Waterloo.
- Al T. A., Martin C. J., and Blowes D. W. (2000) Carbonate-mineral/water interaction in sulfide rich mine tailings. *Geochim. Cosmochim. Acta* 64, 3933–3948.
- Allison J. D., Brown D. S., and Novo-Gradac K. J. (1990) *MINTEQA2/PRODEFA2, a Geochemical Assessment Model for Environmental Systems: Version 3.0 User's Manual*. Environmental Research Laboratory, U.S. Environmental Protection Agency, Athens, GA.
- Ball J. W. and Nordstrom D. K. (1991) *Users Manual for WATEQ4F. With Revised Thermodynamic Data Base and Test Cases for Calculating Speciation of Major Trace, and Redox Elements in Natural Water*. USGS Open-File Report, 91–183. U.S. Geological Survey, Menlo Park, CA.
- Blowes D. W. (1990) *The Geochemistry, Hydrogeology and Mineralogy of Decommissioned Sulfide Tailings: A Comparative Study*. Ph.D. thesis, University of Waterloo.
- Blowes D. W. and Jambor J. L. (1990) The pore-water geochemistry and the mineralogy of the vadose zone of sulfide tailings, Waite Amulet, Quebec, Canada. *Appl. Geochem.* 5, 327–346.
- Blowes D. W. and Ptacek C. J. (1994) Acid-neutralization mechanisms in inactive mine tailings. In *The Environmental Geochemistry of Sulfide Mine-Wastes*, Short Course Handbook 22 (eds. D. W. Blowes and J. L. Jambor), pp. 271–292. Mineralogical Association of Canada, Waterloo, Canada.
- Blowes D. W., Reardon E. J., Jambor J. L., and Cherry J. A. (1991) The formation and potential importance of cemented layers in inactive sulfide mine tailings. *Geochim. Cosmochim. Acta* 55, 965–978.
- Boorman R. S. and Watson D. M. (1976) Chemical processes in abandoned sulfide tailings dumps and environmental implications for northeastern New Brunswick. *Can. Inst. Mining Metall. Bull.* 69, 86–96.
- Booth J., Hong Q., Compton R. G., Prout K., and Payne R. M. (1997) Gypsum overgrowths passivate calcite to acid attack. *J. Colloid Interface Sci.* 192, 207–214.
- Coggans C. J. (1992) *Hydrogeology and Geochemistry of the INCO Ltd., Copper Cliff, Ontario, Mine Tailings Impoundments*. M.S. thesis, University of Waterloo.
- Davis J. A., Fuller C. C., and Cook A. D. (1987) A model for trace metal sorption processes at the calcite surface: Adsorption of  $\text{Cd}^{2+}$  and subsequent solid solution formation. *Geochim. Cosmochim. Acta* 51, 1477–1490.
- Dubrovsky N. M. (1986) *Geochemical Evolution of Inactive Pyritic Tailings in the Elliot Lake Uranium District*. Ph.D. thesis, University of Waterloo.
- Dubrovsky N. M., Cherry J. A., and Reardon E. J. (1985) Geochemical evolution of inactive pyritic tailings in the Elliot Lake uranium district. *Can. Geotech. J.* 22, 110–128.
- Dutrizac J. E. and Chen T. T. (1990) A chemical and mineralogical study of silver, lead and cadmium in Kidd Creek zinc concentrates and roaster products. In *Lead-Zinc '90* (eds. T. S. Mackey and R. D. Prengaman), pp. 161–191. The Minerals, Metals & Materials Society, Warrendale, PA.
- Dzombak D. A. and Morel F. M. M. (1990) *Surface Complexation Modeling: Hydrous Ferric Oxide*. John Wiley, New York.
- Felmy A. R. and Weare J. H. (1986) The prediction of borate mineral equilibria in natural waters: Application to Searles Lake, California. *Geochim. Cosmochim. Acta* 50, 2771–2783.
- Fuller C. C. and Davis J. A. (1987) Processes and kinetics of  $\text{Cd}^{2+}$  sorption by a calcareous aquifer sand. *Geochim. Cosmochim. Acta* 51, 1491–1502.
- Gibbs M. M. (1979) A simple method for the rapid determination of iron in natural waters. *Water Res.* 19, 295–297.
- Greenberg A. E., Clesceri L. S., and Eaton A. D. (1992) *Standard Methods for the Examination of Water and Waste Water*, 18th ed. American Health Association.
- Jambor J. L., Owens, D. R., Carriere, P., and Lastra, R. (1993) *Mineralogical Investigation of Tailings and Associated Waste Products, and the Distribution of Natrojarosite in the Kidd Creek Main Tailings Cone, Timmins, Ontario*. MSL 93-20 (CR), 1–198. Canada Center for Mineral and Energy Technology, Mineral Sciences Laboratories Division Report, Ottawa, ON.
- Johnson R. H. (1993) *The Physical and Chemical Hydrogeology of the Nickel Rim Mine Tailings, Sudbury, Ontario*. M.S. thesis, University of Waterloo.
- Johnson R. H., Blowes D. W., Robertson W. D., and Jambor J. L. (2000) The hydrogeochemistry of the Nickel Rim mine tailings impoundment, Sudbury, Ontario. *J. Contam. Hydrol.* 41, 49–80.
- Kinniburgh D. G., Jackson M. L., and Syers J. K. (1976) Adsorption of alkaline earth, transition, and heavy metal cations by hydrous oxide gels of iron and aluminum. *Soil Sci. Soc. Am. J.* 40, 796–799.
- Light T. S. (1972) Standard solution for redox potential measurements. *Anal. Chem.* 44, 1038–1039.
- Morin K. A. and Cherry J. A. (1986) Trace amounts of siderite near a uranium-tailings impoundment, Elliot Lake, Ontario, Canada, and its implication in controlling contaminant migration in a sand aquifer. *Chem. Geol.* 56, 117–134.
- Morin K. A., Cherry J. A., Dave N. K., Lim T. P., and Vivuyurka A. J. (1988) Migration of acidic groundwater seepage from uranium-tailings impoundments, 1. Field study and conceptual hydrogeochemical model. *J. Contam. Hydrol.* 2, 271–303.
- Moses C. O. and Herman J. S. (1991) Pyrite oxidation at circumneutral pH. *Geochim. Cosmochim. Acta* 55, 471–482.
- Nicholson R. V., Gillham R. W., and Reardon E. J. (1988) Pyrite oxidation in carbonate-buffered solution: I. Experimental kinetics. *Geochim. Cosmochim. Acta* 52, 1077–1085.
- Nordstrom D. K. (1977) Thermochemical redox equilibria of ZoBell's solution. *Geochim. Cosmochim. Acta* 41, 1835–1841.
- Nordstrom D. K., Alpers C. N., Ptacek C. J., and Blowes D. W. (2000) Negative pH and extremely acidic mine waters from Iron Mountain, California. *Environ. Sci. Technol.* 34, 254–258.
- Nordstrom D. K., Plummer N. L., Langmuir D., Busenberg E., May H. M., Jones B. P., and Parkhurst D. L. (1990) Revised chemical equilibrium data for major water-mineral reactions and their limitations. In *Chemical Modeling of Aqueous Systems II*, ACS Symposium Series 416 (eds. D. C. Melchior and R. L. Bassett), pp. 398–413. American Chemical Society, Washington, DC.
- Papelis C., Hayes K. F., and Leckie J. O. (1988) *HYDRAQL: A Program for the Computation of Chemical Equilibrium Composition of Aqueous Batch Systems Including Surface-Complexation Modeling of Ion Adsorption at the Oxide/Solution Interface*. Technical Report 306, 1–130. Stanford University, Stanford, CA.
- Parker J. C. and van Genuchten M. T. (1994) Determining transport parameters from laboratory and field tracer experiments. *Virginia Agricultural Experiment Station Bulletin* 84-3, 1–97. Department of Agronomy, Virginia Polytechnic Institute and State University, Blacksburg.
- Ptacek C. J. (1992) *Experimental Determination of Siderite Solubility in High Ionic-Strength Aqueous Solutions*. Ph.D. thesis, University of Waterloo.



- Ptacek C. J. and Gillham R. W. (1992) Laboratory and field measurements of non-equilibrium transport in the Borden aquifer, Ontario, Canada. *J. Contam. Hydrol.* 10, 119-158.
- Ptacek, C. J., Moncur, M., McGregor, R., Blowes, D. W. (2001) Geochemical controls on metal concentrations in mine tailings that have undergone 50 years of oxidation. In *Eleventh Ann. V. M. Goldschmidt Conference*, Abstract #3647, LPI Contribution No. 1088, Lunar and Planetary Institute, Houston, TX (CD-ROM).
- Reardon E. J. (1970) Complexing of silica by iron(III) in natural waters. *Chem. Geol.* 25, 339-345.
- Ribet I., Ptacek C. J., Blowes D. W., and Jambor J. L. (1995) The potential for metal release by reductive dissolution of weathered mine tailings. *J. Contam. Hydrol.* 17, 239-273.
- Singer P. C. and Stumm W. (1970) Acid mine drainage: The rate-determining step. *Science* 167, 1121-1123.
- Stipp S. L., Hochella M. F., Jr., Parks G. A., and Leckie J. O. (1992)  $\text{Cd}^{2+}$  uptake by calcite, solid-state diffusion, and the formation of solid solution: Interface processes observed with near-surface sensitive techniques (XPS, LEED, and AES). *Geochim. Cosmochim. Acta* 56, 1941-1954.
- Stumm W. and Morgan J. J. (1996) *Aquatic Chemistry*, 3rd ed. John Wiley, New York.
- Thorpe R. E., Pringle G. J., and Plant A. G. (1976) Occurrence of selenide and sulphide minerals in bornite ore of the Kidd Creek massive sulphide deposit, Timmins, Ontario. Report of Activities, Part A. Paper 76-1A, 311-317. Geological Survey of Canada, Ottawa, ON.
- U.S. Environmental Protection Agency. (1994) *Acid Mine Drainage Prediction* (530-R-94-036). U.S. Environmental Protection Agency, Washington, DC.

Environment Canada Library, Burlington  
  
3 9055 1018 1942 2



Environment  
Canada

Environnement  
Canada

Canada

**Canada Centre for Inland Waters**

P.O. Box 5050  
867 Lakeshore Road  
Burlington, Ontario  
L7R 4A6 Canada

**National Hydrology Research Centre**

11 Innovation Boulevard  
Saskatoon, Saskatchewan  
S7N 3H5 Canada

**St. Lawrence Centre**

105 McGill Street  
Montreal, Quebec  
H2Y 2E7 Canada

**Place Vincent Massey**

351 St. Joseph Boulevard  
Gatineau, Quebec  
K1A 0H3 Canada

**Centre canadien des eaux intérieures**

Case postale 5050  
867, chemin Lakeshore  
Burlington (Ontario)  
L7R 4A6, Canada

**Centre national de recherche en hydrologie**

11, boul. Innovation  
Saskatoon (Saskatchewan)  
S7N 3H5 Canada

**Centre Saint-Laurent**

105, rue McGill  
Montreal (Quebec)  
H2Y 2E7 Canada

**Place Vincent-Massey**

351 boul. St-Joseph  
Gatineau (Quebec)  
K1A 0H3 Canada